Synthesis, Structures, and Thermal Stability of Dialkyl and Bis(amido) Zirconium(IV) Acen Complexes

Majeda Al Hareri[a] and David J. H. Emslie*,[a]

[a] Department of Chemistry
McMaster University
1280 Main St West, Hamilton, ON, L8S 4M1, Canada
E-mail: emslied@mcmaster.ca
Supporting information for this article is given via a link at the end of the document.

Abstract: Reaction of one equivalent of H_2(acen), H_2(*cis*-Cyacen) or H_2(*trans*-Cyacen) with [Zr(CH_2SiMe_3)$_4$] at room temperature afforded [Zr(acen)(CH_2SiMe_3)$_2$] (**1**), [Zr(*cis*-Cyacen)(CH_2SiMe_3)$_2$] (**2**) or [Zr(*trans*-Cyacen)(CH_2SiMe_3)$_2$] (**3**), respectively (acen = C_2H_4(NCMeCHC(O)Me)$_2$; Cyacen = 1,2-C_6H_{10}(NCMeCHC(O)Me)$_2$). These alkyl compounds are trigonal prismatic in the solid state, and whereas **1** and **3** decomposed without sublimation above 120 °C (5-10 mTorr), **2** sublimed in >95% yield at 85 °C (5-10 mTorr). However, heating solid **2** at 88 °C under static argon for 24 hours resulted in extensive decomposition to afford H_2(cis-Cyacen) and $SiMe_4$ as the soluble products. Compound **2** reacted cleanly with two equivalents of ^{t}BuOH to afford [Zr(*cis*-Cyacen)(O^{t}Bu)$_2$] (**4**), but excess ^{t}BuOH caused both $SiMe_4$ and H_2(*cis*-Cyacen) elimination. The 1:1 reaction of H_2(acen) with [Zr(NMeEt)$_4$] did not proceed cleanly, and 8-coordinate [Zr(acen)$_2$] (**5**) was identified as a by-product; this complex was isolated from the 2:1 reaction. A zirconium amido complex, [Zr(acen)(NMeEt)$_2$] (**6**) was accessed via the reaction of **1** with two equiv. or excess HNMeEt, but decomposed readily in solution at room temperature. More sterically hindered [Zr(acen){N($SiMe_3$)$_2$}$_2$] (**7**) was synthesized via the reaction of [Zr(acen)Cl_2] with two equivalents of Li{N($SiMe_3$)$_2$}, but was also thermally unstable as a solid and in solution at room temperature. Compounds **1**-**3**, **5** and **7** were crystallographically characterized.

Introduction

Acen^R ligands are tetradentate dianions featuring two β-ketiminate units, with the general formula [1,2-C_2R_x(NCR'CR''C(O)R''')$_2$]$^{2-}$, where the CR''CR''' unit is not part of an aromatic ring (from herein, acen^R is used to refer to ligands with any substitution pattern, whereas acen is used to refer only to C_2H_4(NCMeCHC(O)Me)$_2$). They have been used to prepare a broad range of complexes from throughout the periodic table.[1-7] Previously reported zirconium acen^R complexes include [(acen^R)ZrCl_2], [(acen^R)ZrCl_2(THF)],[8] [(acen^R)Zr($CH_2{}^t$Bu)$_2$][9] (acen^R = acen or acen-F_6 {C_2H_4(NCMeCHC(O)CF_3)$_2$}) and [Zr(acen-F_6)$_2$],[10] as well as cationic alkyl derivatives such as [(acen-F_6)Zr($CH_2{}^t$Bu)L_x][B(C_6F_5)$_4$] (L = NMe_2Ph, PMe_2Ph, PMe_3 or NCMe).[9]

As part of a project focused on atomic layer deposition (ALD)[11-14] of zirconium-containing thin films, we became interested in zirconium(IV) complexes in which two *trans*-disposed anionic ligands might be selectively removed by protonation by an alcohol or amine, and we considered that [(acen^R)ZrR_2] (R = alkyl or amido) complexes could be suitable candidates. For use in ALD, precursor molecules should be sufficiently volatile for delivery into the reactor in the vapour phase (typically at a pressure between 0.1 and 1 Torr), and thermally stable enough to withstand weeks of heating at the delivery temperature. Consequently, we set out to prepare [(acen^R)ZrR_2] (R = alkyl or amido) complexes bearing acen {1,2-C_2H_4(NCMeCHC(O)Me)$_2$} ligands, due to their low molecular weight, and *cis*- and *trans*-Cyacen ligands (Scheme 1), given that the more rigid *cis*- or *trans*-1,2-disubstituted cyclohexane linker might be expected to afford complexes with enhanced thermal stability. A phenylene linker would perhaps have a similar effect, but such ligands were not pursued due to the propensity of aryl rings to engage in π-stacking, resulting in decreased volatility.

Several acen^R complexes have previously been utilized as CVD (chemical vapour deposition) or ALD precursors. For example, [Cu(acen)] has been used, in combination with H_2 or O_2 to deposit metallic copper or copper oxide thin films by MOCVD,[15,16] [Ni(acen)] has been employed for the deposition of elemental nickel films as well as Ni/TiO_2 and Ni/CrN composite thin films by plasma-assisted MOCVD,[17,18] and [Ga(acen)H], [Ga(acen-Ph_2)(Me)] (acen-Ph_2 = C_2H_4(NCMeCHC(O)Ph)$_2$), and [Al(acen)(O^{i}Pr)] have been investigated as precursors for gallium and aluminium oxide deposition by aerosol-assisted chemical vapour deposition.[19,20] Additionally, [Zr(acen-F_6)$_2$] was found to be an effective MOCVD precursor for the growth of yttrium-stabilized ZrO_2 using Y(tmhd)$_3$ (tmhd = tetramethylheptanedionate) as the co-precursor and H_2O-saturated N_2O gas as the co-reactant.[21]

Results and Discussion

Reaction of one equivalent of H_2(acen), H_2(*cis*-Cyacen) or H_2(*trans*-Cyacen) with [Zr(CH_2SiMe_3)$_4$] at room temperature afforded red [Zr(acen)(CH_2SiMe_3)$_2$] (**1**), dark yellow [Zr(*cis*-Cyacen)(CH_2SiMe_3)$_2$] (**2**) or yellow [Zr(*trans*-Cyacen)(CH_2SiMe_3)$_2$] (**3**), respectively (Scheme 1).

X-ray quality crystals of **1** were obtained from toluene/hexanes at –30 °C. The crystal structure of **1** (Figure 1) revealed a distorted trigonal prismatic coordination geometry, with each triangular face consisting of a nitrogen, an oxygen, and a carbon donor atom. This geometry was assigned based on the smaller continuous shape measurement (CSM) value of 1.58 for trigonal prismatic geometry versus 11.53 for octahedral geometry (Table 1). Consistent with this geometry, the twist angles (α; c in Figure 1) are 6.49°, 6.98° and 23.89°, which are much closer to 0° (expected for a trigonal prism) than to 60° (expected for an octahedron). Zirconium is approximately equidistant from the two triangular faces (Zr-centroid = 1.380 and 1.389 Å), and the angle between the planes of the two NO-chelates within the acen ligand is 36.8°.

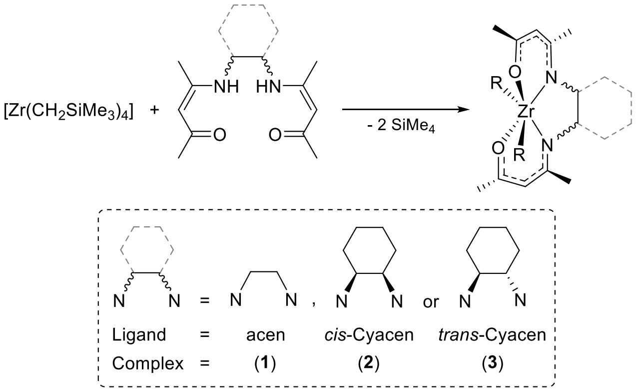

Scheme 1. Synthesis of dialkyl complexes **1**-**3** by $SiMe_4$ elimination.

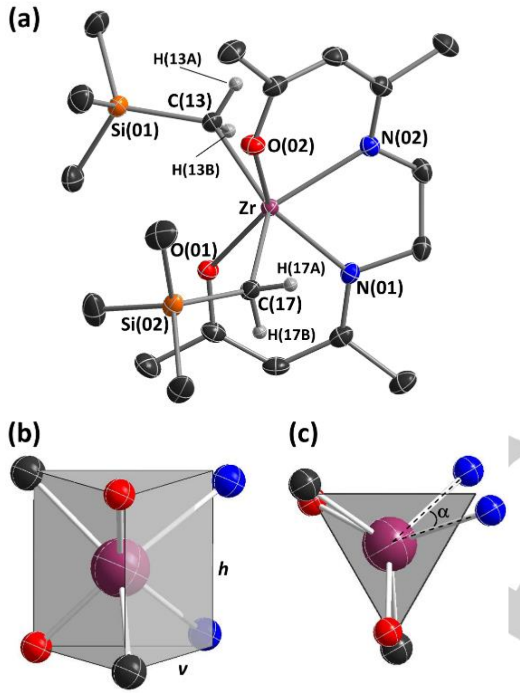

Figure 1. (a) X-ray crystal structure of $[Zr(acen)(CH_2SiMe_3)_2]$ (**1**) with ellipsoids at 50% probability. The Zr-CH_2 hydrogen atoms were located from the difference map and refined isotropically; all other hydrogen atoms are omitted for clarity. Selected bond lengths (Å) and angles (°): Zr-O(01) 2.096(1), Zr-O(02) 2.107(1), Zr-N(01) 2.275(1), Zr-N(02) 2.268(1), Zr-C(13) 2.265(1), Zr-C(17) 2.280(1), N(01)-Zr-N(02) 74.19(4), C(13)-Zr-C(17) 139.96(5), Zr-C(13)-Si(01) 129.58(7), Zr-C(17)-Si(02) 128.25(7), Zr-C(13)-H(13A) 103(1), Zr-C(13)-H(13B) 100(1), Zr-C(17)-H(17A) 100(1), Zr-C(17)-H(17B) 100(1). (b)-(c) Coordination geometry around Zr in **1** superimposed on the ideal trigonal prism calculated by the SHAPE program.

The Zr–C distances {2.265(1) and 2.280(2) Å} are within the usual range for 6-coordinate zirconium bis(trimethylsilylmethyl) complexes {2.224(3)-2.36(2) Å}, whereas the Zr–C–Si bond angles of 128.25(7)° and 129.58(7)° lie at the upper end of the reported range {113.96(8)-127.8(2)°},[22] likely due to steric hindrance or the presence of α-agostic interactions. The $^1J_{C,H}$ NMR coupling constant for **1** is 106 Hz, which is at the upper end of the range for early transition metal and f-element complexes for which α-agostic interactions have been proposed,[23-29] and the Zr–C–H angles {100(1)°} are not especially acute, more consistent with a steric origin for the moderately expanded Zr–C–Si angle.[30-36] For comparison, the $^1J_{C,H}$ NMR coupling constants for $[(acen^R)Zr(CH_2CMe_3)_2]$ ($acen^R$ = acen-F_6 or acen) are 109.8 and 112.5 Hz, respectively, and the Zr–C–C angles in the solid state structure of the former complex are 124.7(3)° and 128.1(3)°.[9]

Table 1. Comparison of the continuous shape measure (CSM) values for trigonal prismatic (TPR-6) and octahedral (OC-6) geometry and twist angles of complexes **1**-**3** and **7**, as well as crystallographically characterized literature examples of 6-coordinate zirconium(IV) $acen^R$ complexes.

Complex	**TPR-6 CSM**	**OC-6 CSM**	**Twist angles, α (°)[a]**
1	1.576	11.532	6.49, 6.98, 23.89[b]
2	1.645	15.785	3.19, 3.23, 18.67[b]
3	4.459 5.465	11.225 10.911	8.40, 9.36, 35.78[b] 9.80, 10.89, 39.41[b]
7	3.472	8.508	7.84[b], 27.93, 27.93
$[Zr(acen)Cl_2]$[8]	11.242	3.141	37.85, 44.38, 50.17
$[Zr(acen\text{-}F_6)(CH_2{}^tBu)_2]$[9]	1.348	15.446	0.01, 3.98, 17.28[b]
$[Zr(acen\text{-}F_6)(CH_2{}^tBu)(NMe_2Ph)][B(Ar^F)_4]$[9]	7.371	7.540	18.45, 24.73, 49.07[b]

[a] The ideal twist angles for a trigonal prism are 0°, compared with 60° for an octahedron. [b] Twist angle associated with the N donor atoms.

Additionally, the Zr–O {2.097(1) and 2.107(1) Å} and Zr–N {2.268(1) and 2.275(1) Å} distances are within the range for previously reported 6-coordinate Zr $acen^R$ complexes {Zr–O = 1.977(3)-2.138(3); Zr–N = 2.217(4)-2.347(4)}.[8,9] In comparison to isostructural $[Zr(acen\text{-}F_6)(CH_2{}^tBu)_2]$, complex **1** features shorter Zr–O, Zr–N, and Zr–C bonds, consistent with reduced steric hindrance, and a more obtuse C–Zr–C bond angle.[9]

Pale yellow, needle-like crystals of **2** and yellow block crystals of **3** were obtained from concentrated hexanes solutions at –30 °C. The structure of **2** (Figure 2a) is analogous to that of **1**, with similar CSM and α values (Table 1), Zr–C {2.281(2) and 2.288(2) Å}, Zr–O {2.110(1) and 2.135(1) Å} and Zr–N {2.273(1) and 2.290(1) Å} distances, and slightly less obtuse Zr–C–Si angles {119.74(8)° and 120.11(8)°; $^1J_{C,H}$ is 105 Hz}. Compound **3** (Figure 2b) is also trigonal prismatic, but differs significantly from **1** and **2** in that the Zr, N and O atoms lie approximately in a plane. The angle between the planes of the two NO-chelates within the *trans*-Cyacen ligand is 70.4 and 69.3° in the two molecules in the unit cell, and the Zr–C {2.251(1)-2.294(1) Å}, Zr–O {2.120(1)-2.143(1)}, and Zr–N {2.236(1)-2.288(2) Å} distances and Zr–C–Si angles {123.71(7)-125.74(7)} are similar to those in **1** and **2** ($^1J_{C,H}$ is ~110 Hz for **3**).

Complexes **1**-**3** formed pale to vivid yellow solutions when dissolved in benzene or toluene. Complex **1** has approximate C_2 symmetry in the solid state, but gave rise to single $N(CH_2)_2N$ and $ZrCH_2$ environments in the ^1H NMR spectrum, indicative of apparent C_{2v} symmetry in solution, presumably due to a fluxional process involving trigonal prismatic and octahedral structures as shown in Scheme 2. The $ZrCH_2$ ^1H and ^{13}C NMR signals for **1** were observed at 0.18 ppm and 54.61 ppm, respectively. By contrast, **2** is C_1 symmetric, and the two trimethylsilylmethyl groups are inequivalent at room temperature and below, giving rise (at 298 K) to broad $ZrCH_2$ signals at 0.39 and 0.21 ppm in the

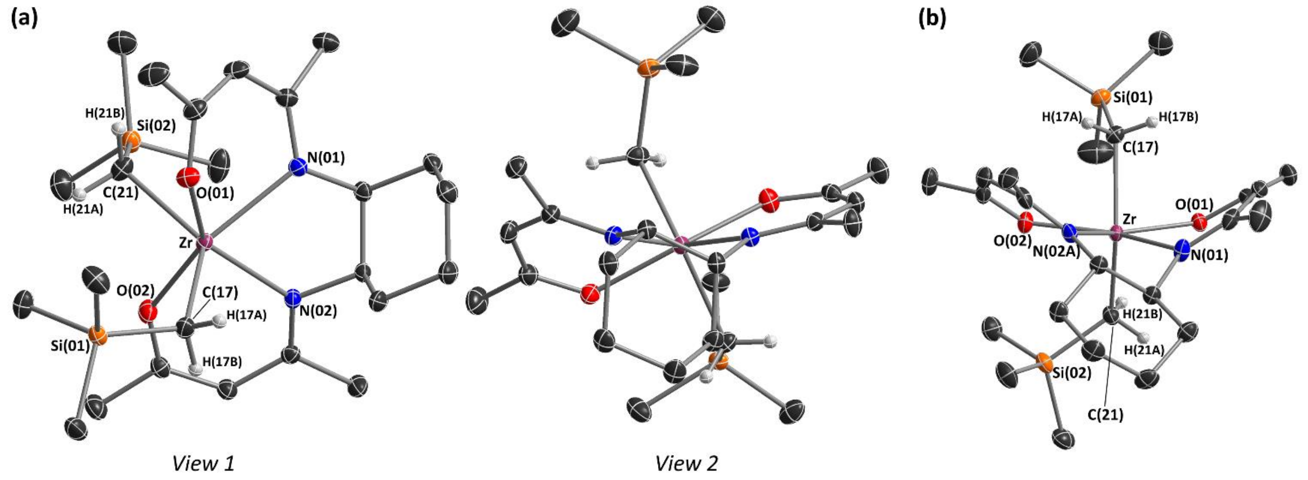

Figure 2. X-ray crystal structures of (a) [Zr(*cis*-Cyacen)(CH_2SiMe_3)$_2$] (**2**; two views are shown to facilitate comparison of the structure of **2** with those of **1** and **3**) and (b) [Zr(*trans*-Cyacen)(CH_2SiMe_3)$_2$] (**3**; only one of two independent and essentially isostructural molecules in the unit cell is shown; both molecules in the unit cell displayed disorder at the cyclohexyl ring, one nitrogen donor atom, and one of the *trans*-Cyacen ligand's CH_3 and CH groups). Ellipsoids are set at 50% probability. The Zr-CH_2 hydrogen atoms were located from the difference map and refined isotropically; all other hydrogen atoms have been omitted for clarity. Selected bond lengths (Å) and angles (°) for **2**: Zr-O(01) 2.135(1), Zr-O(02) 2.110(1), Zr-N(01) 2.273(1), Zr-N(02) 2.290(1), Zr-C(17) 2.281(2), Zr-C(21) 2.288(2), N(01)-Zr-N(02) 72.55(4), C(17)-Zr-C(21) 127.09(6), Zr-C(17)-Si(01) 120.11(8), Zr-C(21)-Si(02) 119.73(8), Zr-C(17)-H(17A) 105(2), Zr-C(17)-H(17B) 105(2), Zr-C(21)-H(21A) 102(2), Zr-C(21)-H(21B) 109(2). Selected bond lengths (Å) and angles (°) for **3**: Zr-O(01) 2.143(1), Zr-O(02) 2.129(1), Zr-N(01) 2.235(1), Zr-N(02A) 2.288(1), Zr-C(17) 2.251(1), Zr-C(21) 2.278(1), N(01)-Zr-N(02A) 70.38(6), C(17)-Zr-C(21) 135.70(5), Zr-C(17)-Si(01) 125.74(7), Zr-C(21)-Si(02) 124.32(7), Zr-C(17)-H(17A) 100(1), Zr-C(17)-H(17B) 104(1), Zr-C(21)-H(21A) 100(1), Zr-C(21)-H(21B) 105(1).

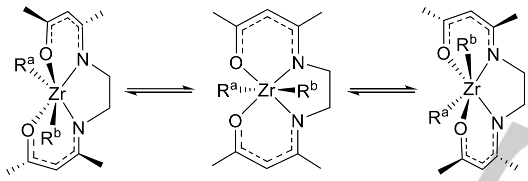

Scheme 2. Isomerization, involving interconversion between trigonal prismatic and octahedral structures, proposed to explain the apparent C_{2v} symmetry of compound **1** in solution at room temperature. The two equivalent alkyl groups are labelled R^a and R^b.

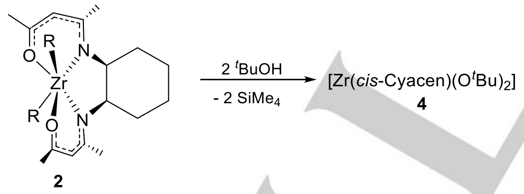

Scheme 3. Reaction of **2** with ^{t}BuOH to afford [Zr(*cis*-Cyacen)(O^{t}Bu)$_2$] (**4**).

^{1}H NMR spectrum, and 57.02 and 54.78 ppm in the ^{13}C NMR spectrum. At high temperature (348 K), the two trimethylsilylmethyl groups were rendered equivalent by an unidentified fluxional process. At low temperature (188 K) the two NC*H* and C*H*(CMe)$_2$ environments became inequivalent, presumably due to slowing of a fluxional process involving ring flip of the cyclohexane ring in the ligand backbone. Conversely, **3** has approximate C_2 symmetry at room temperature, but the ZrCH_2 protons are diastereotopic, affording doublets ($^2J_{H,H}$ = 10.6 Hz) at 0.31 and 0.12 ppm in the ^{1}H NMR spectrum, and a single ^{13}C NMR signal at 56.39 ppm.

Compound **2** reacted cleanly with 2 equivalents of ^{t}BuOH to afford [Zr(*cis*-Cyacen)(O^{t}Bu)$_2$] (**4**; Scheme 3), which was characterized in solution, demonstrating that the alkyl groups could be selectively removed by protonation. However, reaction of **2** with excess ^{t}BuOH resulted in both $SiMe_4$ and H$_2$(*cis*-Cyacen) formation. The volatility and thermal stability of **1**-**3** was evaluated by attempted sublimation at 5-10 mTorr. Compounds **1** and **3** decomposed without sublimation at 140 and 130 °C, respectively. By contrast, compound **2** sublimed in >95% yield at 85 °C. However, heating pure **2** at 88 °C under static argon for 24 hours resulted in extensive decomposition to afford H$_2$(*cis*-Cyacen) and $SiMe_4$ as the soluble products, indicating that **2** lacks the long-term thermal stability typically required for an ALD precursor.

As a potential means to improve the thermal stability of the target precursors, bis-amido Zr(IV) acen^R complexes were pursued in place of dialkyl complexes. Initial attempts to synthesize such complexes via amine elimination proved unsuccessful. For example, reaction of H$_2$(acen) and [Zr(NMeEt)$_4$] in a 1:1 molar ratio resulted in a mixture of products, one of which was identified as [Zr(acen)$_2$] (**5**; *vide infra*). Reactions of [Zr(NMeEt)$_4$] with 1 equiv. of *cis*- or H$_2$(*trans*-Cyacen) also yielded multiple unidentified products, as did reactions of [(acen)ZrCl$_2$] with 2 equiv. of LiNMeEt.

Complex **5** was formed in good yield from the 2:1 reaction of H$_2$acen with either [Zr(CH_2SiMe_3)$_4$] or [Zr(NMeEt)$_4$] (Scheme 4), and yellow-orange single crystals of **5** were obtained from toluene at –30 °C (complex **5** could also be purified by sublimation). This complex features two κ^4-coordinated acen ligands (Figure 3), zirconium and the N and O donors of each acen ligand lie approximately in a plane, and the angle between the ONNO planes of the two ligands is nearly orthogonal (87.8°), analogous to the bonding situation in [Zr(acen-F$_6$)$_2$] (88.5°).[10] The geometry of **5** is intermediate between square antiprismatic and triangular dodecahedral, but the structure is not of sufficient quality for more detailed discussion of bond metrics.

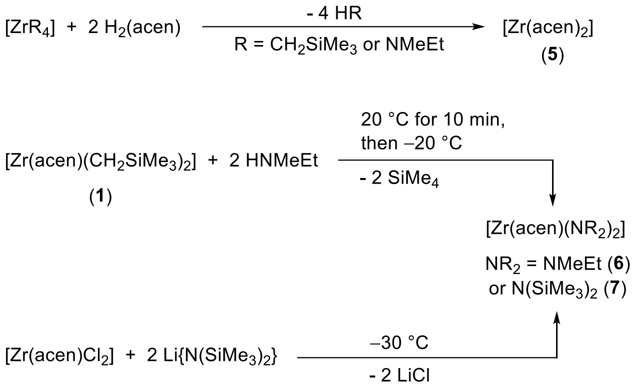

Scheme 4. Syntheses of $[Zr(acen)_2]$ (**5**) and the bis(amido) complexes $[Zr(acen)(NMeEt)_2]$ (**6**) and $[Zr(acen)\{N(SiMe_3)_2\}_2]$ (**7**).

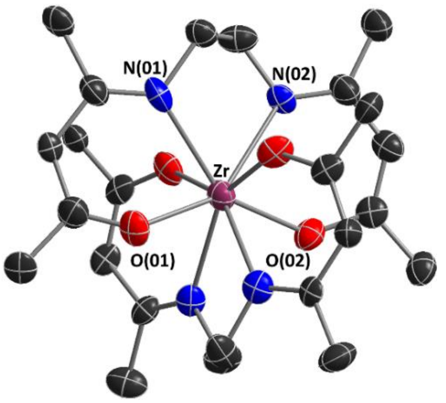

Figure 3. X-ray crystal structure of $[Zr(acen)_2]$ (**5**) with ellipsoids set at 50% probability and all hydrogen atoms omitted for clarity.

The target $[Zr(acen)(NMeEt)_2]$ complex, **6**, was ultimately synthesized via the reaction of excess HNMeEt with $[Zr(acen)(CH_2SiMe_3)_2]$ (**1**) in C_6D_6 or d_8-toluene (Scheme 4). When this reaction was carried out at room temperature, partial product decomposition was evident after 30 minutes (even when only 2 equivalents of HNMeEt were used in the reaction). However, **6** was generated cleanly by stirring at room temperature for 10 minutes in d_8-toluene followed by cooling to –20 °C or below, enabling in-situ characterization by ^1H and ^{13}C NMR spectroscopy (Figures S17 and S18). The thermal instability of **6** is surprising, and attempts to isolate or obtain X-ray quality crystals of **6** were unsuccessful.

In an effort to access a bis-amido complex with increased thermal stability, a more sterically encumbered bis(trimethylsilyl)amido analogue of **6** was pursued. Compound **1** failed to react with excess $HN(SiMe_3)_2$ at room temperature or 50 °C. By contrast, reaction of $[Zr(acen)Cl_2]$ with 2 equiv. of $Li\{N(SiMe_3)_2\}$ at –30 °C afforded the target product, $[Zr(acen)\{N(SiMe_3)_2\}_2]$ (**7**; Scheme 4), which was isolated by crystallization at –30°C. Compound **7** is thermally unstable both as a solid and in solution at room temperature. However, it was characterized by ^1H, ^{13}C and ^{29}Si NMR spectroscopy at 249 K in d_8-THF, revealing one singlet for the NCH_2CH_2N protons, one $SiMe_3$ environment, and one *CH* signal, presumably due to a fluxional process analogous to that proposed for dialkyl complex **1** (Scheme 2).

Large yellow crystals of **7** were obtained from toluene/hexanes at –30 °C. The structure features a κ^4-coordianted acen ligand and two bis(trimethylsilyl)amido ligands, affording a distorted trigonal prismatic geometry (Figure 4; Table 1). The twist angles of the prism are 7.84, 27.93, and 27.93°, but unlike $acen^R$ complexes **1**-**3**, the smallest twist angle is associated with the NCH_2CH_2N bridge as a consequence of a larger angle of 73.5° between the planes of the two NO-chelates within the $acen^R$ ligand (cf. 36.8° in **1**). This likely arises to alleviate unfavourable steric interactions between the acen dianion and the bulky amido ligands. Consistent with significant steric hindrance in compound **7**, the N(02)–Zr–N(02') angle between the amido groups (114.87(4)°) is far more acute than the 139.96(5)° C–Zr–C angle between the alkyl groups in **1**. Nevertheless, the $Zr–N_{acen}$ and Zr–O distances in **7** {2.3271(8) and 2.1435(6) Å, respectively} are only marginally longer than those in **1**, and the $Zr–N_{amido}$ bond distance in **7** {2.1242(7) Å} falls within the typical range for $Zr–N(SiMe_3)_2$ linkages {2.020(2) – 2.180(3) Å}.[37]

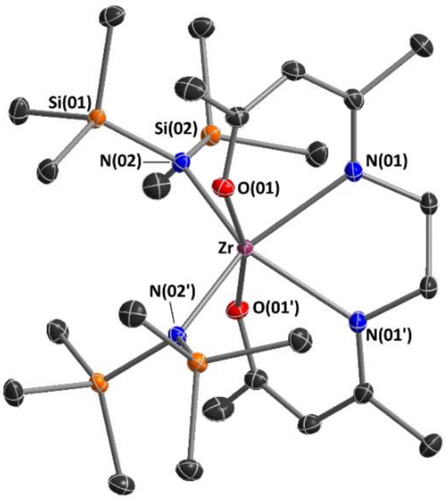

Figure 4. X-ray crystal structure of $[Zr(acen)\{N(SiMe_3)_2\}_2]$ (**7**) with ellipsoids set at 50% probability and hydrogen atoms omitted for clarity. Selected bond lengths (Å) and angles (°): Zr-O(01) 2.1435(6), Zr-N(01) 2.3271(8), Zr-N(02) 2.1242(7), N(01)-Zr-N(01') 69.61(4), N(02)-Zr-N(02') 114.87(4), Zr-N(02)-Si(01) 124.85(4), Zr-N(02)-Si(02) 118.87(4).

Summary and Conclusions

This work presents the synthesis of reactive dialkyl and bis(amido) zirconium complexes employing acen, *cis*-Cyacen and *trans*-Cyacen ligands. Key findings include: (a) the *cis*-Cyacen ligand afforded a zirconium dialkyl complex with greater thermal stability and volatility than the acen or *trans*-Cyacen analogues; the *cis*-Cyacen compound sublimed cleanly at 85 °C *in vacuo*, (b) the $acen^R$ dialkyl complexes are significantly more thermally robust than the acen bis(amido) complexes, which decomposed at room temperature; the unexpectedly low thermal stability of these complexes may explain the absence of group 4 bis(amido) $acen^R$ complexes in the literature, (c) in the solid state, the dialkyl and bis(amido) complexes are best described as trigonal prismatic rather than octahedral, although fluxional NMR behaviour indicates facile access to octahedral structures in solution, (d) the $acen^R$ ligand in zirconium dialkyl complexes is susceptible to protonlysis even by weakly acidic reagents such as

^{t}BuOH, limiting the potential of such complexes for ALD involving selective reactivity at the monodentate ligands, (e) reaction of one equiv. of H_2(acen) with [Zr(NMeEt)$_4$] failed to cleanly generate [(acen)Zr(NMeEt)$_2$], although this product could be accessed cleanly via the reaction of [(acen)Zr(CH_2SiMe_3)$_2$] with two or more equiv. of HNMeEt; by contrast, [(acen)Zr(CH_2SiMe_3)$_2$] did not react with excess HN($SiMe_3$)$_2$, even at 50 °C, and (f) reaction of [(acen)ZrCl_2] with two equiv. of LiNMeEt afforded a mixture of unidentified products, whereas the analogous reaction with Li{N($SiMe_3$)$_2$} generated [(acen)Zr{N($SiMe_3$)$_2$}$_2$] in high yield, highlighting the sensitivity of these reactions to the nature of the amido ligand.

Experimental Section

General Details: All reactions of newly prepared complexes were conducted under an atmosphere of argon. An argon-filled Innovative Technology PureLab HE glovebox equipped with a −30 °C freezer was employed for the manipulation and storage of all oxygen- and moisture-sensitive compounds. Air-sensitive syntheses were performed on a double-manifold high-vacuum line (with mercury bubblers) equipped with an Edwards R12 vacuum pump using standard Schlenk techniques. The vacuum was measured periodically using a Kurt J. Lesker 275i convection enhanced Pirani gauge. Commonly utilized specialty glassware included thick-walled flasks equipped with Teflon taps leading to a 24/40 glass joint (bombs), or J. Young or Wilmad LPV NMR tubes. Centrifugation was performed using a Fisher Scientific model 228 centrifuge [using Kimble 15 mL glass centrifuge tubes (21020-684) and Wheaton PTFE-lined phenolic caps (240463)] located within the glovebox. Argon cylinders (Linde) of 99.998% and 99.999% purity were used for the vacuum lines, respectively. Argon supplied to the vacuum lines was purified to below 0.1 ppm of O_2 and 0.5 ppm H_2O using an Oxisorb-W scrubber from Matheson Gas Products.

Hexanes, toluene, THF, and deuterated benzene were purchased from Sigma-Aldrich. Deuterated toluene and THF were purchased from Cambridge Isotope Laboratories. All solvents were initially dried over an appropriate drying agent (hexanes and THF = Na/Ph_2CO/tetraglyme; toluene = Na; C_6D_6, d_8-toluene, d_8-THF = Na/Ph_2CO), and then distilled. $ZrCl_4$, Zr(NMeEt)$_4$, $LiCH_2SiMe_3$ (1.0M in pentane) ethylenediamine, *cis*- and *trans*-1,2-diaminocyclohexane, acetylacetone, ethylmethylamine, methyllithium (1.6M in Et_2O), hexamethyldisilazane, Li{N($SiMe_3$)$_2$}, and *tert*-butanol were purchased from Sigma-Aldrich. $ZrCl_4$ was stored under argon and freshly sublimed before each use. Ethylmethylamine and *t*-butanol were dried using 4Å mol. sieves, degassed, and stored under argon in a storage flask. All other reagents were used without further purification. H_2(acen), [Zr(acen)Cl_2], and [Zr(CH_2SiMe_3)$_4$], were prepared using literature procedures.[8,38] LiNMeEt was prepared by the addition of HNMeEt to a solution *n*-BuLi in hexanes at –78 °C and the removal of all volatiles after stirring at room temperature overnight to obtain the desired product as a white solid. *Cis*- and H_2(*trans*-Cyacen) were prepared using the same method as H_2(acen) (similar to the previously reported method, but starting with pure *cis*- or *trans*-1,2-diaminocyclohexane).[39] The proligands H_2(acen), H_2(*cis*-Cyacen), and H_2(*trans*-Cyacen) were dissolved in toluene and dried over 4Å molecular sieves for 2 weeks before use.

Solution NMR spectroscopy was performed on a Bruker AV-600 spectrometer at 298 K and a Bruker AV-500 spectrometer between 188 and 348 K. All ^{1}H and ^{13}C NMR spectra were referenced relative to $SiMe_4$ through the resonance of the protio impurity in C_6D_6, d_8-toluene, and d_8-THF (for ^{1}H NMR; 7.16, 2.11 (CH_3), and 3.58 (OCH_2) ppm, respectively) or the resonance of each solvent (for ^{13}C NMR; 128.06, 20.43 (CD_3), and 67.21 (OCD_2) ppm, respectively). ^{29}Si NMR spectra were indirectly referenced by conversion of the spectral frequency of the ^{1}H NMR spectrum using the frequency ratio of ^{1}H and ^{29}Si, as described by Harris *et al*.[40]

Combustion elemental analyses were performed at the University of Calgary using a Perkin Elmer Model 2400 series II analyzer. Single crystal X-ray diffraction studies were conducted on crystals coated in Paratone oil and mounted on either a SMART APEX II diffractometer with a 3 kW sealed-tube Mo generator and SMART6000 CCD detector, or on a STOE IPDS II diffractometer with an image plate detector in the McMaster Analytical X-ray (MAX) diffraction facility. Raw data was processed using XPREP (as part of the APEX v2.2.0 software) and solved by an intrinsic method (SHELXT).[41,42] In all cases, non-hydrogen atoms were refined anisotropically and hydrogen atoms were generated in ideal positions and then updated with each refinement cycle (except for all ZrCH_2 hydrogen atoms in complexes **1**-**3** which were located from the difference map and refined isotropically). All structure solutions and refinements were performed using Olex2.[43] Geometries were assigned through the use of continuous shape measure (CSM) analysis using the SHAPE program.[44]

CCDC 2208417 (for **1**), 2208418 (for **2**), 2208419 (for **3**), 2208420 (for **5**), and 2208421 (for **7**) contain the supplementary crystallographic data for this paper. These data can be obtained free of charge from the Cambridge Crystallographic Data Centre.

[Zr(acen)(CH_2SiMe_3)$_2$] (1): A solution of H_2(acen) (116 mg, 0.52 mmol) in toluene (10 mL) was added dropwise to a solution of [Zr(CH_2SiMe_3)$_4$] (228 mg, 0.52 mmol) in hexanes (5 mL) at room temperature, whereupon the clear, pale yellow solution turned bright yellow in colour. The reaction darkened to a clear, red solution while stirring overnight at room temperature. Volatiles were removed *in vacuo* to obtain a dark red solid that was >95% pure by NMR spectroscopy (229 mg, 89%). Analytically pure and X-ray quality single crystals were grown by layering hexanes onto a saturated toluene solution (1:3) and cooling to –30 °C (95 mg, 38%). Compound **1** decomposed without sublimation at 140 °C. No decomposition was observed by NMR spectroscopy after heating solid **1** at 120 °C *in vacuo* for 6 hours. ^{1}H NMR (C_6D_6, 500 MHz, 298K): δ 5.27 (s, 2H, C*H*), 3.02 (s, 4H, NCH_2), 2.16 (s, 6H, CH_3CO), 1.50 (s, 6H, CH_3CN), 0.29 (s, 18H, CH_2Si(CH_3)$_3$), 0.18 (s, 4H, CH_2SiMe_3) ppm. ^{13}C{^{1}H} NMR (C_6D_6, 126 MHz, 298K): δ 181.44 (*C*=O), 171.63 (*C*=N), 102.68 (*C*H), 54.61 (*C*H_2SiMe_3), 53.07 (N*C*H_2), 25.50 (*C*H_3CO), 22.94 (*C*H_3CN), 3.38 (CH_2Si(*C*H_3)$_3$) ppm. ^{29}Si NMR (C_6D_6, 99 MHz, 298 K): δ −3.7 ppm.[45] $C_{20}H_{40}N_2O_2Si_2Zr$ (487.95 g mol^{-1}): calcd. C 49.23, H 8.26, N 5.74%; found. C 49.36, H 8.09, N 6.00%.

[Zr(*cis*-Cyacen)(CH_2SiMe_3)$_2$] (2): A solution of H_2(*cis*-Cyacen) (131.6 mg, 0.47 mmol) in toluene (10 mL) was added dropwise to a solution of [Zr(CH_2SiMe_3)$_4$] (208.1 mg, 0.47 mmol) in hexanes (5 mL) at room temperature, whereupon the clear, pale yellow solution turned bright yellow in colour. Volatiles were removed *in vacuo* after stirring at room temperature overnight. A dark yellow powder was obtained that was >95% pure by NMR spectroscopy (220 mg, 86%). Analytically pure and X-ray quality single crystals were grown from a concentrated hexanes solution at –30 °C as pale yellow needles (107 mg, 42%). Compound **2** sublimed in >95% yield at 85 °C. However, heating **2** at 88 °C under static argon for 24 hours resulted in extensive decomposition to afford H_2(*cis*-Cyacen) and $SiMe_4$ as the soluble products. ^{1}H NMR (C_6D_6, 600 MHz, 298K): δ 5.29 (s, 2H, C*H*), 3.66 (m, 2H, NC*H*), 2.18 (s, 6H, CH_3CO), 1.71 (m, 2H) and 1.04 (m, 2H, CH_2CH_2CH), 1.63 (s, 6H, CH_3CN), 1.21 (m, 2H) and 0.94 (m, 2H, C$H_2$$CH_2$CH), 0.49 and 0.12 (2 bs, 18H, CH_2Si(CH_3)$_3$), 0.39 and 0.21 (2 bs, 4H, CH_2SiMe_3) ppm. ^{13}C{^{1}H} NMR (C_6D_6, 151 MHz, 298K): δ 180.90 (*C*=O), 171.22 (*C*=N), 103.81 (*C*H), 62.72 (N*C*H), 57.02 and 54.78 (*C*H_2SiMe_3), 31.13 (CH_2*C*H_2CH), 25.40 (*C*H_3CO), 22.87 (*C*H_3CN), 22.38 (*C*$H_2$$CH_2$CH), 3.41 ($CH_2$Si(*C*$H_3$)$_3$) ppm. ^{29}Si NMR ($d_8$-toluene, 99 MHz, 238 K): δ −4.01 and −3.53 ppm.[45] $C_{24}H_{46}N_2O_2Si_2Zr$ (542.04 g mol^{-1}): calcd. C 53.18, H 8.55, N 5.17%; found. C 53.17, H 8.36, N 5.40%.

[Zr(*trans*-Cyacen)(CH_2SiMe_3)$_2$] (3): A solution of H_2(*trans*-Cyacen) (210.1 mg, 0.48 mmol) in toluene (10 mL) was added dropwise to a solution of [Zr(CH_2SiMe_3)$_4$] (132.9 mg, 0.48 mmol) in hexanes (10 mL) at room temperature, whereupon the clear, pale yellow solution turned bright yellow in colour. Volatiles were removed *in vacuo* after stirring at room temperature overnight. A yellow powder was obtained that was >95% pure by NMR spectroscopy (220 mg, 90%). Analytically pure and X-ray quality single crystals were grown from a concentrated hexanes solution at –30 °C as yellow blocks (126 mg, 49%). Compound **3** decomposed without sublimation at 130 °C. No decomposition was observed by NMR spectroscopy after heating solid **3** at 120 °C *in vacuo* for 6 hours. ^{1}H NMR (C_6D_6, 500 MHz, 298K): δ 5.23 (s, 2H, C*H*), 3.36 (m, 2H, NC*H*), 2.23 (s, 6H, C*H*$_3$CO), 1.67 (m, 2H) and 1.18 (m, 2H, CH$_2$C*H*$_2$CH), 1.62 (s, 6H, C*H*$_3$CN), 1.31 (m, 2H) and 0.80 (m, 2H, C*H*$_2$CH$_2$CH), 0.39 (s, 18H, CH$_2$Si(C*H*$_3$)$_3$), 0.31 and 0.12 (2 d, 2×2H, $^2J_{H,H}$ = 10.6 Hz) ppm. ^{13}C{^{1}H} NMR (C_6D_6, 126 MHz, 298K): δ 181.20 (*C*=O), 169.12 (*C*=N), 104.08 (*C*H), 66.14 (N*C*H), 56.39 (*C*H$_2$SiMe$_3$), 33.31 (CH$_2$*C*H$_2$CH), 25.64 (*C*H$_3$CO), 25.62 (*C*H$_2$CH$_2$CH), 23.38 (*C*H$_3$CN), 3.62 (CH$_2$Si(*C*H$_3$)$_3$) ppm. ^{29}Si NMR (C_6D_6, 99 MHz, 298 K): δ −3.8 ppm.[45] $C_{24}H_{46}N_2O_2Si_2Zr$ (542.04 g mol^{-1}): calcd. C 53.18, H 8.55, N 5.17%; found. C 53.75, H 8.71, N 5.21%.

[Zr(*cis*-Cyacen)(O^{t}Bu)$_2$] (4): A solution of **2** (15.5 mg, 0.028 mmol) dissolved in C_6D_6 (0.4 mL) was prepared in a NMR tube sealed with a rubber septum and parafilm. A 0.52M solution of *t*-butanol in C_6D_6 (0.12 mL, 0.063 mmol) was added via syringe through the rubber septum. Upon addition, the pale yellow solution instantly became colourless, and complete conversion of **2** to **4** was observed by NMR spectroscopy. ^{1}H NMR (C_6D_6, 500 MHz, 298K): δ 5.01 (s, 2H, C*H*), 3.60 (bs, 2H, NC*H*), 2.41 (m, 2H) and 1.29 (m, 2H, CH$_2$C*H*$_2$CH), 1.98 (s, 6H, C*H*$_3$CO), 1.65 (s, 6H, C*H*$_3$CN), 1.52 (m, 2H) and 1.12 (m, 2H, C*H*$_2$CH$_2$CH) ppm, 1.39 (s, 18H, OC(C*H*$_3$)$_3$) ppm. ^{13}C{^{1}H} NMR (C_6D_6, 126 MHz, 298K): δ 179.21 (*C*=O), 169.70 (*C*=N), 102.89 (*C*H), 74.35 (O*C*(CH$_3$)$_3$), 60.65 (N*C*H), 32.90 (OC(*C*H$_3$)$_3$), 30.41 (CH$_2$*C*H$_2$CH), 25.63 (*C*H$_3$CO), 22.30 (*C*H$_2$CH$_2$CH), 21.66 (*C*H$_3$CN) ppm.

[Zr(acen)$_2$] (5): A solution of [Zr(NMeEt)$_4$] (139.3 mg, 0.43 mmol) in toluene (5 mL) was added dropwise to a solution of H$_2$(acen) (193.1 mg, 0.86 mmol) in toluene (10 mL) at room temperature. The yellow solution was stirred at room temperature for 2 days and turned red. Volatiles were removed *in vacuo*, and the solid residue was washed with hexanes and then dried *in vacuo* to obtain a red solid that was >95% pure by NMR spectroscopy (170 mg, 74%). Analytically pure and X-ray quality single crystals were grown from a concentrated toluene solution at –30 °C as yellow-orange needles (68 mg, 29%). Complex **5** could also be purified by sublimation at 105 °C at 10 mTorr, and no decomposition was detected by NMR after heating solid **5** for 24 hours under static argon at 145 °C. ^{1}H NMR (C_6D_6, 600 MHz, 298K): δ 4.86 (s, 4H, C*H*), 3.80 (s, 8H, NC*H*$_2$), 1.75 (s, 12H, C*H*$_3$CO), 1.71 (s, 12H, C*H*$_3$CN) ppm. ^{13}C{^{1}H} NMR (C_6D_6, 151 MHz, 298K): δ 172.02 (*C*=O), 162.97 (*C*=N), 100.38 (*C*H), 51.82 (N*C*H$_2$), 25.03 (*C*H$_3$CO), 22.24 (*C*H$_3$CN) ppm. $C_{24}H_{36}N_4O_4Zr$ (535.80 g mol^{-1}): calcd. C 53.80, H 6.77, N 10.46%; found. C 54.14, H 6.90, N 10.38%.

[Zr(acen)(NMeEt)$_2$] (6): A solution of **1** (13.2 mg, 0.027 mmol) in d_8-toluene was prepared in a NMR tube sealed with a rubber septum secured with parafilm. A 1.16M solution of HNMeEt in C_6D_6 (0.09 mL, 0.105 mmol) was added via syringe through the rubber septum. The mixture was allowed to react at room temperature for 10 minutes and then immersed in a –78 °C cold bath before inserting into an NMR spectrometer held at –20 °C. ^{1}H NMR (d_8-toluene, 500 MHz, 249K): δ 5.28 (s, 2H, C*H*), 3.21 (s, 4H, NC*H*$_2$C*H*$_2$N), 2.97 (q, 4H, NC*H*$_2$CH$_3$), 2.67 (s, 6H, NC*H*$_3$), 1.97 (s, 6H, C*H*$_3$CO), 1.74 (s, 6H, C*H*$_3$CN), 1.02 (t, 6H, NCH$_2$C*H*$_3$) ppm. ^{13}C{^{1}H} NMR (d_8-toluene, 126 MHz, 249K): δ 171.18 (*C*=O), 165.16 (*C*=N), 102.03 (*C*H), 52.01 (N*C*H$_2$*C*H$_2$N), 51.41 (N*C*H$_2$CH$_3$), 41.11 (N*C*H$_3$), 25.45 (*C*H$_3$CO), 23.03 (*C*H$_3$CN), 14.54 (NCH$_2$*C*H$_3$) ppm.

[Zr(acen){N(SiMe$_3$)$_2$}$_2$] (7): Note: all glassware, solvents, and reagents were cooled to –30 °C before this reaction was conducted. A solution of Li{N(SiMe$_3$)$_2$} (21.7 mg, 0.130 mmol) in toluene (1 mL) was added dropwise to a slurry of [Zr(acen)Cl$_2$] (24.9 mg, 0.065 mmol) in toluene (0.5 mL) at –30 °C in a 4 mL vial. The reaction was shaken approximately every 5 minutes and left at –30 °C until the starting material dissolved and LiCl precipitated. The dark red-orange mixture was filtered through a pasteur pipette packed with glass wool and celite to obtain a clear, vivid red solution. Large, yellow block crystals were obtained by layering the toluene solution with 3 mL of hexanes and storing at –30 °C. (35 mg, 85%). ^{1}H NMR (d_8-THF, 500 MHz, 249K): δ 5.54 (s, 2H, C*H*), 3.69 (s, 4H, NC*H*$_2$), 2.07 (s, 6H, C*H*$_3$CO), 2.06 (s, 6H, C*H*$_3$CN), 0.04 (s, 36H, Si(C*H*$_3$)$_3$) ppm. ^{13}C{^{1}H} NMR (d_8-THF, 126 MHz, 249K): δ 178.84 (*C*=O), 172.32 (*C*=N), 105.86 (*C*H), 53.74 (N*C*H$_2$), 25.37 (*C*H$_3$CO), 23.02 (*C*H$_3$CN), 6.88 (Si(*C*H$_3$)$_3$) ppm. ^{29}Si NMR (d_8-THF, 99 MHz, 242 K): δ −7.3 ppm.[45] $C_{24}H_{54}N_4O_2Si_4Zr$ (634.29 g mol^{-1}): calcd. C 45.45, H 8.58, N 8.88%; found. C 45.16, H 8.36, N 8.91%.

Acknowledgements

D.J.H.E. thanks NSERC of Canada for a Discovery Grant, Intel Corporation for funding support via the Semiconductor Research Corporation, and the Ontario government for an Ontario Research Fund Research Excellence (ORF-RE) grant. M.A.H. thanks NSERC of Canada for funding support via a PGS-D award. We are grateful to Drs. James F. Britten in the McMaster X-ray diffraction facility and Yurij Mozharivskyj for advice and support with X-ray crystallography. A special acknowledgement is given to Dr. Jeffrey S. Price from the Emslie lab for collection of X-ray diffraction data and conducting variable temperature NMR studies during times of restricted access due to Covid-19.

Keywords: Acen Complexes • Alkyl Complexes • Amido Complexes • Chelates • Zirconium

References

[1] F. Corazza, C. Floriani, A. Chiesi-Villa, C. Guastini, S. Ciurli, *J. Chem. Soc. Dalton Trans.* **1988**, 2341-2345.
[2] A. Pasini, M. Gullotti, *J. Coord. Chem.* **1974**, *3*, 319-332.
[3] B. J. Kennedy, K. S. Murray, *Inorg. Chem.* **1985**, *24*, 1552-1557.
[4] B. J. Kennedy, A. C. McGrath, K. S. Murray, B. W. Skelton, A. H. White, *Inorg. Chem.* **1987**, *26*, 483-495.
[5] M. North, C. Young, *Catal. Sci. Technol.* **2011**, *1*, 93-99.
[6] Y.-P. Cai, H.-Z. Ma, B.-S. Kang, C.-Y. Su, W. Zhang, J. Sun, Y.-L. Xiong, *J. Organomet. Chem.* **2001**, *628*, 99-106.
[7] V. Mougel, P. Horeglad, G. Nocton, J. Pécaut, M. Mazzanti, *Chem. Eur. J.* **2010**, *16*, 14365-14377.
[8] F. Corazza, E. Solari, C. Floriani, A. Chiesi-Villa, C. Guastini, *J. Chem. Soc. Dalton Trans.* **1990**, 1335-1344.
[9] E. B. Tjaden, D. C. Swenson, R. F. Jordan, J. L. Petersen, *Organometallics* **1995**, *14*, 371-386.
[10] A. Bastianini, G. A. Battiston, F. Benetollo, R. Gerbasi, M. Porchia, *Polyhedron* **1997**, *16*, 1105-1110.
[11] D. Panda, T.-Y. Tseng, *Thin Solid Films* **2013**, *531*, 1-20.
[12] T.-J. Chang, Y.-S. Jiang, S.-H. Yi, C.-Y. Chou, C.-I. Wang, H.-C. Lin, M.-J. Chen, *Appl. Surf. Sci.* **2022**, *591*, 153110.
[13] B. Yoon, J. L. O'Patchen, D. Seghete, A. S. Cavanagh, S. M. George, *Chem. Vap. Deposition* **2009**, *15*, 112-121.
[14] B. H. Lee, V. R. Anderson, S. M. George, *Chem. Vap. Deposition* **2013**, *19*, 204-212.
[15] T. Gerfin, M. Becht, K.-H. Dahmen, *Mater. Sci. Eng., B* **1993**, *17*, 97-100.
[16] G. G. Condorelli, G. Malandrino, I. L. Fragalà, *Chem. Vap. Deposition* **1999**, *5*, 237-244.
[17] P. A. Premkumar, A. Dasgupta, P. Kuppusami, P. Parameswaran, C. Mallika, K. S. Nagaraja, V. S. Raghunathan, *Chem. Vap. Deposition* **2006**, *12*, 39-45.
[18] S. Arockiasamy, V. S. Raghunathan, P. A. Premkumar, P. Kuppusami, A. Dasgupta, P. Parameswaran, C. Mallika, K. S. Nagaraja, *Chem. Vap. Deposition* **2007**, *13*, 691-697.
[19] D. Pugh, P. Marchand, I. P. Parkin, C. J. Carmalt, *Inorg. Chem.* **2012**, *51*, 6385-6395.
[20] C. E. Knapp, P. Marchand, C. Dyer, I. P. Parkin, C. J. Carmalt, *New J. Chem.* **2015**, *39*, 6585-6592.
[21] J. A. Belot, R. J. McNeely, A. Wang, C. J. Reedy, T. J. Marks, G. P. A. Yap, A. L. Rheingold, *J. Mater. Res.* **1999**, *14*, 12-15.
[22] Bond distance and angle range based on a search of the Cambridge Structural Database for 6-coordinate zirconium bis(trimethylsilylmethyl) complexes.100% of the Zr-C distances

and Zr-C-Si angles in the CSD fall within the range described. CSD accessed via conquest CSD on September 13, 2022; version 5.42, updated November 2020).
[23] J. W. Bruno, G. M. Smith, T. J. Marks, C. K. Fair, A. J. Schultz, J. M. Williams, *J. Am. Chem. Soc.* **1986**, *108*, 40-56.
[24] Z. Guo, D. C. Swenson, R. F. Jordan, *Organometallics* **1994**, *13*, 1424-1432.
[25] A. F. Dunlop-Brière, P. H. M. Budzelaar, M. C. Baird, *Organometallics* **2012**, *31*, 1591-1594.
[26] J. Jaffart, M. Etienne, F. Maseras, J. E. McGrady, O. Eisenstein, *J. Am. Chem. Soc.* **2001**, *123*, 6000-6013.
[27] D. L. Clark, S. K. Grumbine, B. L. Scott, J. G. Watkin, *Organometallics* **1996**, *15*, 949-957.
[28] L. Turculet, T. D. Tilley, *Organometallics* **2002**, *21*, 3961-3972.
[29] C. A. Cruz, D. J. H. Emslie, L. E. Harrington, J. F. Britten, C. M. Robertson, *Organometallics* **2007**, *26*, 692-701.
[30] D. M. Amorose, R. A. Lee, J. L. Petersen, *Organometallics* **1991**, *10*, 2191-2198.
[31] In metal (M) alkyl complexes with CH_2ER_3 (E = Si or C) ligands, the interpretation of expanded M-C-E angles and $^1J_{C,H}$ coupling constants should be approached with caution, given that larger M-C-E angles can arise due to steric effects, potentially giving rise to smaller $^1J_{C,H}$ coupling constants due to decreased s-character in the C-H bonds (see refs. 23 and 24). Furthermore, $^1J_{C,H}$ coupling constants are diminished when the carbon atom is attached to an electropositive substituent, as predicted by Bent's rule (see ref. 32). For example, the $^1J_{C,H}$ coupling for $SiMe_4$ is 118 Hz, compared with 124 Hz for CMe_4 (see ref. 33), and the $^1J_{C,H}$ coupling for the methyl ligands in $[\{MgMe_2(\mu\text{-}1,4\text{-dioxane})\}_n]$ (in d_8-THF) is 106 Hz (see ref. 34), compared with 115.5 Hz for the terminal methyl groups in Al_2Me_6 (see ref. 35), and 125 Hz for methane (see ref. 36).
[32] H. A. Bent, *Chem. Rev.* **1961**, *61*, 275-311.
[33] R. B. Nazarski, W. Makulski, *Phys. Chem. Chem. Phys.* **2014**, *16*, 15699-15708.
[34] R. Fischer, H. Görls, P. R. Meisinger, R. Suxdorf, M. Westerhausen, *Chem. Eur. J.* **2019**, *25*, 12830-12841.
[35] O. Yamamoto, *J. Chem. Phys.* **1975**, *63*, 2988-2995.
[36] N. Muller, D. E. Pritchard, *J. Chem. Phys.* **1959**, *31*, 768-771.
[37] Bond distance range based on a search of the Cambridge Structural Database for zirconium bis(trimethylsilyl)amido complexes. 96% of the Zr-N distances in the CSD fall within the range described. CSD accessed via conquest CSD on September 13, 2022; version 5.42, updated November 2020).
[38] M. R. Collier, M. F. Lappert, R. Pearce, *J. Chem. Soc. Dalton Trans.* **1973**, 445-451.
[39] C. H. Huang, L. F. Hsueh, P. C. Kuo, H. M. Lee, C. L. Uno, J. H. Huang, C. Y. Tu, C. H. Hu, G. H. Lee, C. H. Hung, *Eur. J. Inorg. Chem.* **2008**, *2008*, 3000-3008.
[40] R. K. Harris, E. D. Becker, S. M. C. d. Menezes, R. Goodfellow, P. Granger, *Pure Appl. Chem.* **2001**, *73*, 1795-1818.
[41] G. M. Sheldrick, *Acta Crystallogr. Sect. A: Found. Crystallogr.* **2015**, *71*, 3-8.
[42] G. M. Sheldrick, *Acta Crystallogr. Sect. C: Cryst. Struct. Commun.* **2015**, *71*, 3-8.
[43] O. V. Dolomanov, L. J. Bourhis, R. J. Gildea, J. A. K. Howard, H. Puschmann, *J. Appl. Crystallogr.* **2009**, *42*, 339-341.
[44] H. Zabrodsky, S. Peleg, D. Avnir, *J. Am. Chem. Soc.* **1992**, *114*, 7843-7851.
[45] Chemical shift located from a crosspeak in the 2D ^{29}Si-^1H HMBC NMR spectrum.